

## Rydberg Trimers and Excited Dimers Bound by Internal Quantum Reflection

V. Bendkowsky,\* B. Butscher, J. Nipper, J. B. Balewski, J. P. Shaffer,† R. Löw, and T. Pfau  
5. Physikalisches Institut, Universität Stuttgart, Pfaffenwaldring 57, 70569 Stuttgart, Germany

W. Li, J. Stanojevic, T. Pohl,‡ and J. M. Rost

Max-Planck-Institut für Physik komplexer Systeme, Noethnitzer Strasse 38, 01187 Dresden, Germany

(Received 25 February 2010; published 12 October 2010)

In a combined experimental and theoretical effort we report on two novel types of ultracold long-range Rydberg molecules. First, we demonstrate the creation of triatomic molecules of one Rydberg atom and two ground-state atoms in a single-step photoassociation. Second, we assign a series of excited dimer states that are bound by a so far unexplored mechanism based on internal quantum reflection at a steep potential drop. The properties of the Rydberg molecules identified in this work qualify them as prototypes for a new type of chemistry at ultracold temperatures.

DOI: 10.1103/PhysRevLett.105.163201

PACS numbers: 34.50.Cx, 34.20.Cf

The development of techniques to manipulate ultracold atoms has opened up new avenues for molecular physics. The recent experimental success in producing cold ground-state molecules [1–3] is paving the way towards studying chemistry at ultralow temperatures [4]. This regime also offers unprecedented opportunities for the control of large-scale molecules involving highly excited states [5,6], which hold great promise for such applications due to the high sensitivity of Rydberg atoms to external fields [7]. A particular class of Rydberg molecules arises from binding between a Rydberg and a ground-state atom, which is based solely on low-energy collisions between the Rydberg electron and the ground-state atom [8]. Owing to the large size of Rydberg atoms, binding occurs at extremely long range on the order of several thousand Bohr radii  $a_0$ .

Recently, we proved the existence of these ultralong-range molecules in an ultracold rubidium gas [6]. A simple model with an adjustable  $s$ -wave scattering length was found to reproduce the binding energies of the vibrational ground states for a range of principal quantum numbers. Here, we demonstrate the existence of several additional molecular lines. The observed spectra can be adequately described with Fermi's pseudopotential for local Rydberg electron scattering off the perturbing ground-state atom [9,10] but within a nonperturbative Green's function approach which accounts for the strong collisional couplings between Rydberg state manifolds. Despite the lack of an inner potential barrier, the calculated molecular states have the peculiar property to avoid smaller interatomic distances. As we will show, this is due to internal quantum reflection at a shape resonance of electron-atom scattering. The state of the molecular Rydberg electron is determined by both long-range attraction to its parent ion as well as short-range interaction with the nearby ground-state atom. Within a Born-Oppenheimer approximation we obtain the following Hamiltonian for the molecular Rydberg electron (in a.u.):

$$H = -\frac{\nabla^2}{2} + V_{eA^+}(|\mathbf{r} - \mathbf{R}|) + V_{eA}(\mathbf{r}) \equiv H_A + V_{eA}(\mathbf{r}). \quad (1)$$

$\hat{H}_A$  is the Hamiltonian of the unperturbed Rydberg atom, whose center is located at  $\mathbf{R}$ , and where the molecular axis  $\mathbf{R}$  also defines the quantization axis.  $\hat{V}_{eA}(\mathbf{r})$  accounts for the interaction of the Rydberg electron with the perturbing ground-state atom, which is described by a Fermi-type pseudopotential for electron-atom scattering [9,10], including the first two  $l = 0, 1$  partial waves. Within the Fermi model [9], the molecular interaction of low- $\ell$  Rydberg states is commonly described by the simple first-order perturbative potential [9,10]

$$U^{(1)}(R) = 2\pi A_s |\psi_n(R)|^2 + 6\pi A_p^3 |\nabla \psi_n(R)|^2, \quad (2)$$

where  $\psi_n$  is the unperturbed Rydberg wave function and  $A_{s(p)}(k)$  is the energy-dependent  $s$ - ( $p$ )-wave scattering length. The electron momentum  $k$  depends on the Rydberg energy  $E_n$  through the quasiclassical relation  $E_n = k^2/2 - 1/R$ . This approach yields a simple and intuitive description of the molecular interaction and is typically employed to describe molecules formed with energetically well isolated  $ns$  Rydberg states [8,11]. Even for this case, however, Eq. (2) turns out to be inaccurate at the level of accuracy of the experimental data. Hence, we performed nonperturbative Green's function calculations [12] of the molecular potentials (see [13]).

As an example, we compare the calculated potential energy curves  $U(R)$  with the first-order perturbative potential  $U^{(1)}(R)$  for  $n = 35$  in Fig. 1. As is known for high- $\ell$  Rydberg molecules, Eq. (2) fails in the vicinity of the  $p$ -wave shape resonance [14,15] because the resonance leads to an avoided potential crossing. This curve crossing is crucial for determining the vibrational spectrum of the molecule found in our experiments. Unexpectedly,  $U^{(1)}$  also falls short of more accurate calculations around the outer potential well at  $R = 1900a_0$ . One can, nevertheless,

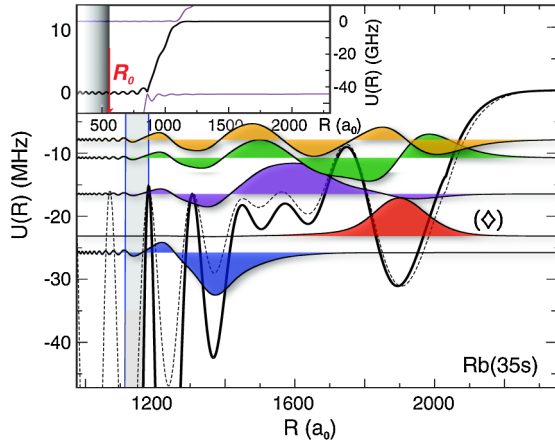


FIG. 1 (color online). Molecular potential curve and wave functions for Rb(35s). Results obtained from the Green's function calculation (solid line) and from the model potential Eq. (2) with an effective scattering length  $A_s^{(\text{eff})} = -19.48a_0$  (dotted line). The gray area at  $R \approx 1200a_0$  marks the innermost badland region defined by  $d\lambda/dR > 1$  [27]. The inset shows the rapid potential drop at the avoided crossing and illustrates the variable inner boundary condition at a distance  $R_0$ .

obtain an approximate description of the strong molecular resonance, localized in the outermost minimum of the potential energy curve, by using an effective, properly adjusted  $s$ -wave scattering length  $A_s^{(\text{eff})}(k=0)$  with Eq. (2) (dotted line in Fig. 1). The corresponding vibrational energy for all principal quantum numbers  $n = 35, 36, 37$  is well reproduced for an effective scattering length of  $A_s^{(\text{eff})} = -19.48a_0$ . While this value is 20% larger than the actual value of  $A_s(k=0)$ , it may serve as an effective parameter or characteristic of a given atomic species that yields the  $n$  dependence of the strongest molecular resonance, based on the simple model potential Eq. (2).

To create the ultralong-range Rydberg molecules, we prepare a cold sample of  $^{87}\text{Rb}$  atoms at  $T = 3 \mu\text{K}$  in the ground state  $5s_{1/2}$ ,  $F = 2$ ,  $m_F = 2$ . The  $ns_{1/2}$  Rydberg atoms with  $n = 35, \dots, 37$  are excited by two narrow-band lasers and subsequently detected by field ionization [6,13]. The vibrational bound dimer and trimer states can be created directly via photoassociation if the detuning of the excitation light from the atomic Rydberg state matches the molecular binding energy  $E_B$ . Therefore, the molecular states appear in the spectra on the red side of the atomic Rydberg line (Fig. 2). The Rb( $ns$ ) spectra consist of two atomic states  $m_s = +1/2(\uparrow)$  and  $m_s = -1/2(\downarrow)$ , separated by the Zeeman splitting  $\Delta_B$  in the magnetic trap, and several molecular lines. The atomic state  $m_s = +1/2(\uparrow)$  and the molecular triplet state  $^3\Sigma(ns-5s)(\uparrow\uparrow)$  have the same Zeeman shift, and thus the binding energy  $E_B$  can be directly measured as the energy difference between the corresponding lines in the spectrum. Note that in our previous work [6] the binding energies  $E_B$  were defined differently. After field ionization, we observe both an atomic ion signal corresponding to  $\text{Rb}^+$  and a molecular

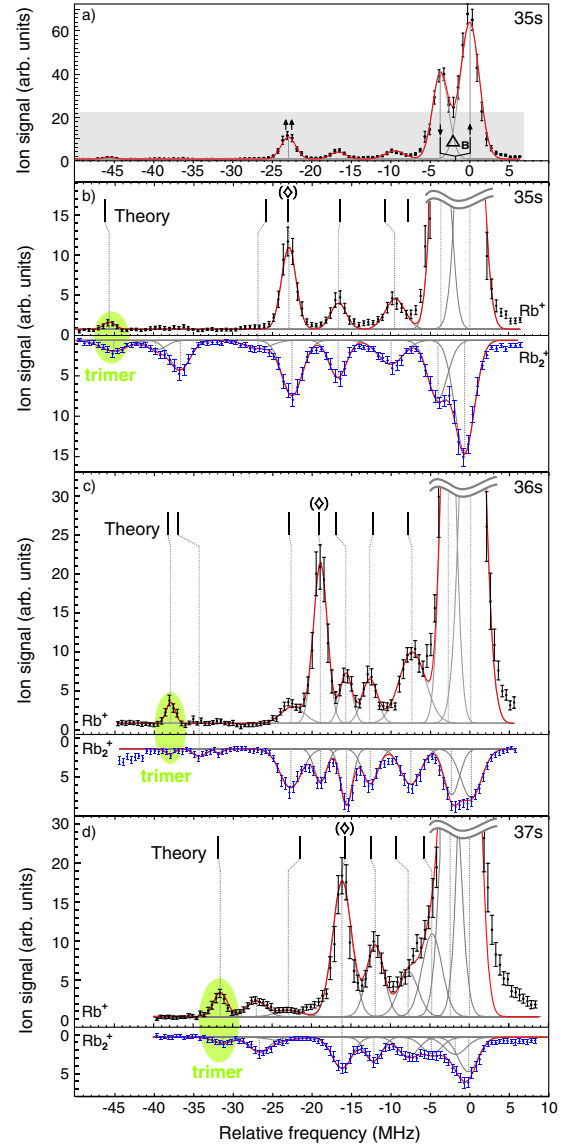


FIG. 2 (color online). Spectra for principal quantum numbers  $n = 35-37$ . (a) Full spectrum for Rb(35s) and illustration of the atomic Zeeman shift  $\Delta_B$ . (b)–(d) Magnified spectra of the states 35s to 37s including statistical errors ( $2\sigma$ ). Frequencies in all spectra are measured with respect to the atomic transition  $5s_{1/2} \rightarrow ns_{1/2}$ . The upper parts show the atomic ion spectrum  $\text{Rb}^+$  and the lower ones the spectra of the molecular ions  $\text{Rb}_2^+$ . Calculated binding energies are indicated by vertical lines.

ion signal corresponding to  $\text{Rb}_2^+$  which can be clearly identified in the time-of-flight spectra. The  $\text{Rb}^+$  and  $\text{Rb}_2^+$  spectra predominantly show the same features but with different intensity distributions. A few deep bound states exclusively appear in the  $\text{Rb}_2^+$  spectrum and can be assigned as dimer states by our theoretical model. The fact that the strengths of the two ion signals are comparable for the molecular states is a clear indication that  $\text{Rb}_2^+$  is the product of an additional decay that occurs for the molecular states. When the long-range bound Rb-Rb pair penetrates to small distances, there are two possible ionization

processes causing  $\text{Rb}_2^+$  formation, namely, Hornbeck-Molnar ionization [16] and  $\text{Rb}^+\text{-Rb}^-$  ion pair formation [17]. Our theoretical description accounts for such loss channels yet predicts the observed molecular resonances independent of the precise nature of the decay process.

To assign the observed lines we employ the *ab initio* data of Refs. [11,14] for the *s*-wave scattering phase shift  $\delta_0(k)$ . Since the available *p*-wave scattering data [11,18] do not yield an accurate description of the measured spectra, we use the modified effective range expression [19] for the corresponding phase shift  $\delta_1$ . This three-parameter fitting procedure allows the assignment of most of the observed lines and reproduces the resonance frequencies with a remarkable accuracy (see Fig. 2). The strongest molecular line in each spectrum, labeled by ( $\diamond$ ), corresponds to the dimer state localized in the outermost potential well (Fig. 1) which was assigned as the vibrational ground state  $\nu = 0$  in Ref. [6]. The present study allows us to identify several additional lines as excited dimer states.

We observe two resonances at deeper binding energy in the experiment. The lowest one systematically appears at twice the binding energy of the outermost localized dimer state ( $\diamond$ ). Three-body potential calculations, using the Green's function approach described above, yield a long-range localized trimer state, which to a high accuracy is bound at twice the energy of the corresponding dimer states ( $\diamond$ ). This provides clear evidence for the direct photoassociation of a long-range triatomic molecule [20,21], in which two ground-state atoms are simultaneously bound to the Rydberg atom via their interaction with the Rydberg electron. The remaining unassigned lines may indicate that excited states of these exotic trimers are also formed in our experiments.

The agreement between theory and experiment confirms existing *s*-wave scattering data, predicting a zero energy *s*-wave scattering length of  $A_s(k=0) = -16.05a_0$  [11,18]. In addition, the described fitting procedure allows us to extract *p*-wave scattering parameters and yields a zero energy scattering length of  $A_p(k=0) = -21.15a_0$ , which is well within the range of previous calculations. Our extracted value for the shape resonance energy  $E_{\text{res}} = 23.6$  meV constitutes the first experimental determination of this quantity and agrees well with theoretical predictions [18,22]. For a pure *s*-wave potential, the outermost localized state ( $\diamond$ ) constitutes the true vibrational ground state of the molecule [6]. A more accurate determination of the molecular potential requires the inclusion of *p*-wave scattering, and, in particular, the shape resonance in the *p*-wave scattering cross section of rubidium [18,22] has to be taken into account, which leads to an avoided crossing between adjacent molecular potential curves around  $\sim 1000a_0$  (inset in Fig. 1). This has a dramatic effect on the vibrational structure and results in additional molecular states that are delocalized over several  $100a_0$  [13] with vibrational energy that lies above the potential maxima inside the attractive potential well. Although energetically

possible, these states have only negligible probability density at interatomic distances smaller than  $\sim 1000a_0$ . As there exists no inner potential barrier that would facilitate a common molecular binding of these excited vibrational states, the binding has to arise from a fundamentally different mechanism. We show that molecular binding in this case originates from quantum reflection at the steep potential drop around  $\sim 1000a_0$ . Because of this enormous potential drop at the avoided crossing, the molecular wave function behaves in the inner region very much like that of a free particle with a relatively large kinetic energy compared to the outermost part of the potential curve. Consequently, the long-range molecular structure is largely unaffected by the details of the interaction at smaller distances. Moreover, the aforementioned decay at small distances acts as an absorber of the wave function and, thus, yields an open boundary condition. Hence, the small leakage into this region can be treated as *inward* scattering—in analogy to standard *outward* scattering problems—such that the molecular states can be obtained from a stabilization procedure [23]. Precisely, we place a reflecting boundary in the inner region of the potential well at  $R_0$  (see the inset in Fig. 1) and record the energy eigenvalues as a function of  $R_0$ . The observed energies are clearly visible in the resulting stabilization plot [Fig. 3(a)] and appear as sharp maxima in the corresponding density of states [Fig. 3(b)].

Within an alternative approach that underlines the crucial role of quantum reflection, we consider an outgoing plane wave injected at  $R = 0$  with an energy below the height of the innermost well. We study the complex reflection coefficient  $\mathcal{R} = |\mathcal{R}|e^{i\Theta}$  of reflection off the outer potential plateau at  $R \sim 1000a_0$ . The scattering phase  $\Theta(E)$  can be related to the time delay  $\tau = d\Theta/dE$  between a scattered and a freely propagating particle [24]. In Fig. 3(c), we show the phase shift for the molecular curve of the  $n = 35$  Rydberg state, while its derivative is depicted by

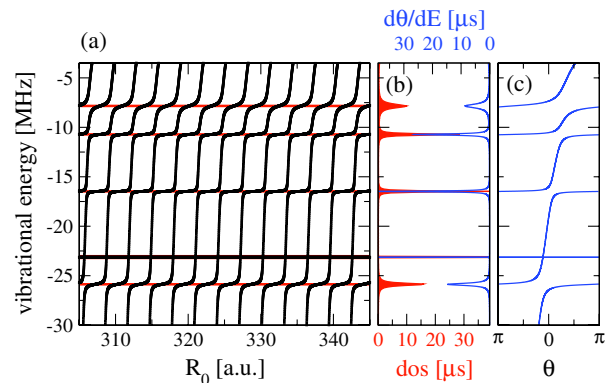


FIG. 3 (color online). (a) Stabilization diagram for  $n = 35$ , showing the vibrational energies as a function of the position of the inner, reflecting boundary at  $R_0$  (see Fig. 1). (b) The corresponding density of states yields the energies and widths of the molecular resonances, in perfect agreement with the results obtained from the reflection phase (c).

the right curve in Fig. 3(b). The energy dependence of  $\tau(E)$  exhibits a small background due to classical slowdown of the outgoing particle, moving up the potential hill. In perfect agreement with the calculated density of states [Fig. 3(b)] we find a series of sharp resonances riding on top of this background. Consequently, these resonances are of nonclassical origin and mark the occurrence of a quasibound state. The resonance line shape is of Breit-Wigner type and, according to Wigner's time delay interpretation, yields the lifetime of the corresponding quasibound state. Such quasibound states occur, e.g., in strong-field ionization of atoms and molecules [25] and affect transport in semiconductors [26], where states are confined inside a well by a high tunneling barrier. In marked contrast to such systems, the presented long-range vibrational states arise nearly entirely from quantum reflection keeping the ground-state atom outside the potential drop. To distinguish the purely quantum mechanics-based reflection from such semiclassical phenomena, the spatial variation of the de Broglie wavelength  $\lambda = 2\pi/\sqrt{2M[E - U(r)]}$  has to be considered [27]. A slow variation of  $\lambda$  defines the semiclassical region. Depending on the vibrational energy, this condition is violated, i.e.,  $d\lambda/dr > 1$ , around the potential maxima in the outer plateau region. Indeed the innermost of these "badlands" extends deep into the left of the sharp potential drop. To identify the dominant contributions of the molecular curve, we adapted the method of Ref. [28] to determine the reflection coefficient of the two inner potential maxima. Even for the highest lying excited state for Rb(35s), the reflection coefficient is as high as  $|\mathcal{R}| \geq 0.7$ . This clearly demonstrates that these unique vibrational states arise from the special form of the interaction potential leading to quantum reflection near the deep abyss at the avoided potential crossing.

The remarkably good agreement between experiment and theory over a range of principal quantum numbers attests to the accuracy of Fermi's original pseudopotential approach in describing interactions in highly excited multiatom systems. A nonperturbative approach of these interactions is, however, necessary and leads to an unusual binding caused by internal quantum reflection. It prevents collapse of the excited dimer states to small interatomic distances, which would lead to fast decay of the molecule. Since the molecular structure is found to be sensitive to the characteristics of both *s*-wave and *p*-wave scattering, long-range Rydberg molecules are an accurate experimental platform to investigate electron-atom collision in a previously inaccessible ultralow-energy domain. The universality of this binding mechanism makes a new type of ultracold Rydberg chemistry feasible: Larger polymers or even heteronuclear molecules can be realized, where the number of atoms, the constituent atomic elements, and the addressed Rydberg state allow for the precise selection of the properties of the long-range molecule. Indeed, the three-body photoassociation demonstrated in this work

may be regarded as an initiating step towards the production of larger and more complex polyatomic molecules.

We thank I. Fabrikant, H. Sadeghpour, and F. Robicheaux for helpful discussions. B.B. thanks the Carl Zeiss foundation and J.P.S. the Humboldt foundation for financial support. Parts of this work are funded by the Deutsche Forschungsgemeinschaft (DFG) within the SFB/TRR21 and Project No. PF 381/4-1.

\*v.bendkowsky@physik.uni-stuttgart.de

†Present address: University of Oklahoma, Homer L. Dodge Department of Physics and Astronomy, 440 W. Brooks Street, Norman, OK 73019, USA.

\*tpohl@pks.mpg.de

- [1] K. K. Ni *et al.*, *Science* **322**, 231 (2008).
- [2] J. G. Danzl *et al.*, *Science* **321**, 1062 (2008).
- [3] J. Deiglmayr *et al.*, *Phys. Rev. Lett.* **101**, 133004 (2008).
- [4] R. V. Krems, *Int. Rev. Phys. Chem.* **24**, 99 (2005).
- [5] K. R. Overstreet *et al.*, *Nature Phys.* **5**, 581 (2009).
- [6] V. Bendkowsky *et al.*, *Nature (London)* **458**, 1005 (2009).
- [7] I. Lesanovsky, P. Schmelcher, and H. R. Sadeghpour, *J. Phys. B* **39**, L69 (2006).
- [8] C. H. Greene, A. S. Dickinson, and H. R. Sadeghpour, *Phys. Rev. Lett.* **85**, 2458 (2000).
- [9] E. Fermi, *Nuovo Cimento* **11**, 157 (1934).
- [10] A. Omont, *J. Phys. (Paris)* **38**, 1343 (1977).
- [11] A. A. Khuskivadze, M. I. Chibisov, and I. I. Fabrikant, *Phys. Rev. A* **66**, 042709 (2002).
- [12] S. P. Andreev *et al.*, *Sov. Phys. JETP* **59**, 506 (1984).
- [13] See supplementary material at <http://link.aps.org/supplemental/10.1103/PhysRevLett.105.163201> for further discussions of the setup and calculations.
- [14] E. L. Hamilton, C. H. Greene, and H. R. Sadeghpour, *J. Phys. B* **35**, L199 (2002).
- [15] C. H. Greene *et al.*, *Phys. Rev. Lett.* **97**, 233002 (2006).
- [16] L. Barbier and M. Cheret, *J. Phys. B* **20**, 1229 (1987).
- [17] M. Cheret *et al.*, *J. Phys. B* **15**, 3463 (1982).
- [18] C. Bahrim and U. Thumm, *Phys. Rev. A* **61**, 022722 (2000).
- [19] T. F. O'Malley, L. Spruch, and L. Rosenberg, *J. Math. Phys. (N.Y.)* **2**, 491 (1961).
- [20] I. C. H. Liu and J. M. Rost, *Eur. Phys. J. D* **40**, 65 (2006).
- [21] I. C. H. Liu, J. Stanojevic, and J. M. Rost, *Phys. Rev. Lett.* **102**, 173001 (2009).
- [22] A. R. Johnston and P. D. Burrow, *J. Phys. B* **15**, L745 (1982).
- [23] A. U. Hazi and H. S. Taylor, *Phys. Rev. A* **1**, 1109 (1970).
- [24] E. P. Wigner, *Phys. Rev.* **98**, 145 (1955).
- [25] G. N. Gibson, G. Dunne, and K. J. Bergquist, *Phys. Rev. Lett.* **81**, 2663 (1998).
- [26] M. Büttiker, *Electronic Properties of Multilayers and Low-dimensional Semiconductor Structures* (Plenum, New York, 1990).
- [27] R. Côté, H. Friedrich, and J. Trost, *Phys. Rev. A* **56**, 1781 (1997).
- [28] Ph. Gossel and J.-M. Vigoureux, *Phys. Rev. A* **55**, 796 (1997).